Nonlinear Finite Element Analysis of Reinforced Concrete Corner Joints Subjected to Opening Moments

David A. M. Jawad
Lecturer, Dept. of Civil Engineering, University of Basrah.
Lateef N. Assi
Asst. Lecturer, Dept. of Building Construction, Muthana Institute of Technology.

Abstract: The study investigates the behaviour of reinforced concrete corner joints under monotonically increasing loads which tend to increase the right angle between the two joint members. The experimental results for two case studies are considered, and the ANSYS computer code is employed to create three-dimensional models for corner joints within the context of the finite element method. The effect of reinforcement details at the corner joint is studied for commonly used detailing systems, and the nonlinear response is traced throughout the entire load range up to failure. The results obtained are generally in good agreement with the experiments, and show that the detailing system has a significant effect on corner joint behaviour, with efficiencies ranging from as low as 54% up to 147%.

Keywords: Corner joints, Concrete, Nonlinear analysis, Finite element method, ANSYS.

التحليل اللاخطي بأستخدام طريقة العناصر المحددة للمفاصل الركنية من الكونكريت المسلح المعرضة الى عزوم فتح

د.ديفد عبد محمد جواد
مدرس- قسم الهندسة المدنية- جامعة البصرة
السيد لطيف ناجح عاصي
مدرس مساعد- قسم البناَء والأنشاءات- المعهد الفني في المثنى

الخلاصة:

يتناول البحث سلوك المفاصل الركنية من الخرسانة المسلحة تحت تأثير أحمال متزايدة والتي تؤدي الى أنفراج قيمة الزاويةالقائمـة بين ضلعي المفصل الركني. تم تناول النتائج العملية لحالتين بحثيتين، وتوظيف برنامج ANSYS في أنشاء نمـاذج ثلاثيـة البعد للمفاصل الركنية ضمن محتوى طريقة العناصر المحددة. جرت دراسة لتأثير تفاصيل التسليح المستخدمة للمفاصل الركنية لبعض أنظمة التسليح الأكثر شيوعا، مع تتبع للأستجابة اللاخطية لمدى التحميل الكلي وصولا للفشل.

االنتائج المستحصلة أظهرت توافقا جيدا مع النتائج العملية وبينت أن تفصيل التسليح ذو تـأثير مهم على سلوك المفصل الركنـي، وبقيم لكفاءة المفصل تتباين من ٥٤% لغاية ١٤٧%.

1. Introduction:

The term "corner" is used to describe a corner joint formed by the joining, at 90°, of the ends of two flexural members. The terms "opening" and "closing" of the corner are used to describe the increase and decrease of this right angle, respectively. Some examples, shown in Fig.(1) include retaining walls, liquid storage tanks and large box culverts.
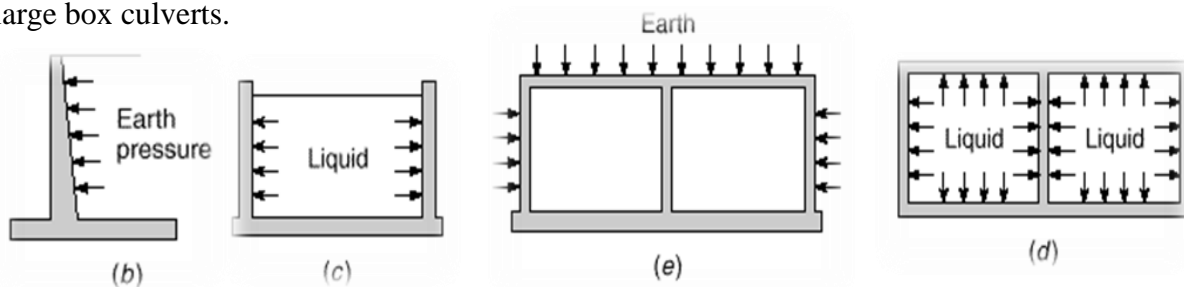
or corners. The reinforcement details must be such that its layout and fabrication is easy and the structural member should satisfy the fundamental requirements of strength expressed in terms of joint efficiency, controlled cracking, ductility and last but not the least, ease and simplicity of construction.

Fig.1 Examples of Corner Joints.

From a safety point of view, it is important that a reinforced concrete structure, apart from necessary load capacity, is also able to show ductile behaviour so that a local failure does not lead to total collapse of the structure [1]. A structure's ability to exhibit such behaviour is highly dependent on the reinforcement detail of the joint connections between its adjoining members. Ideally, the joint should resist a moment at least as large as the estimated failure moment of the structural members connected to it and ensure ductile behaviour in the ultimate limit state.

The principles of detailing and the structural behaviour of simple structural members such as beams and columns are well established. On the other hand, the detailing, strength and behaviour of corner joints, especially those subject to opening moments as in the case of cantilever retaining walls, bridge abutments, channels, rectangular liquid retaining structures and portal frames, has not been conclusively determined. Reinforcement detailing at corners plays a primary role in influencing the structural behaviour of the joint more so in the case of opening joints

Various detailing systems have been popular from time to time and considerable efforts have been directed towards carrying out improvements in these detailing systems to achieve the desired structural behaviour.

2. Stress Analysis:
a-Stress Analysis according to Theory of Elasticity

The state of stress in corners and joints as calculated by the theory of elasticity is valid only before cracking occurs. After cracking and at later stages, the joint acts as a composite structure made up by the reinforcement and the concrete. Thus the analysis of joint behavior is far more complicated than that of homogeneous bodies. Despite the fact that the results provided by the theory of elasticity are valid only prior to cracking, they help to indicate where tensile stresses occur. From an elastic analysis some guidance regarding the location of tension reinforcement in corners and joints is provided [2]. Fig.(2) shows the stress distribution along the diagonal in a corner subjected to positive moment. The bending stress, σ_x, exhibits a peak tension at the inside of the corner, which explains why

corner cracks occur for quite small loads. The tensile stresses, σ_y, cause a diagonal crack across the corner which results in sudden failure unless reinforcement is provided. These tensile stresses may be considered parabolically distributed perpendicular to the joint diagonal Fig.(3). In the shown system of forces, the resultant tensile force across the diagonal is $\sqrt{2}\,F_t = \sqrt{2}\,F_c$. For the parabolic distribution

$$\sqrt{2}\,F_s = \frac{2}{3} f_t\, b\, l_{dc} \quad ...(1)$$

in which f_t = tensile strength of the concrete; b= width of the corner; and l_{dc} = length of the diagonal crack. The bending moment on the corner is $M = Fz$, in which z= lever arm=0.8d; d=effective depth of the member framing in the corner; thus

$$M = F_s\, 0.8d \quad ...(2)$$

Equating (1) and (2) gives:

$$M = \frac{\sqrt{2}}{3} 0.8d\, b\, l_{dc}\, f_t = 0.38 d\, b\, l_{dc}\, f_t \quad ...(3)$$
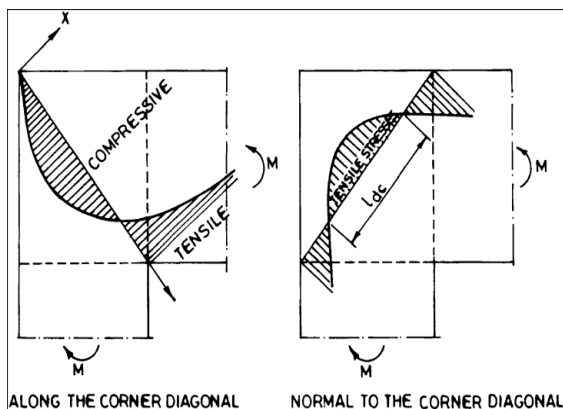
Fig.2 Stress in Corner according to Theory of Elasticity.[2]

b-Stress Analysis according to Strut-and-Tie Model [3]

Although the Committee 352 report [4] is an important contribution to the safe design of joints of certain standard configurations, the recommendations are
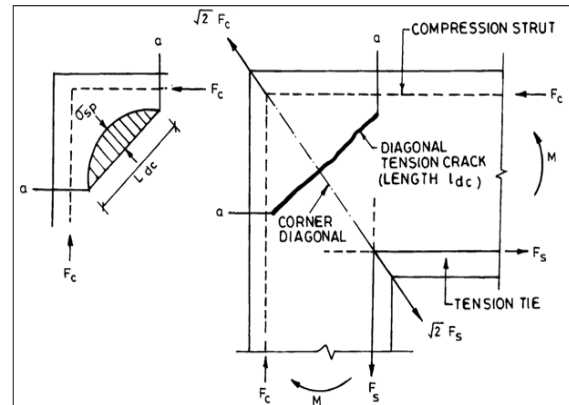

Fig.3 Truss Idealisation of Corner.[2]

based mainly on results of tests. Consequently they must be restricted to joints whose geometry closely matches that of tested joints. This leads to many seemingly arbitrary geometric limitations. Good physical models are available for many aspects of reinforced concrete behavior-for example, for predicting the flexural strength of a beam or the strength of an eccentrically loaded column-but no clear physical model is evident in the Committee 352 recommendations for the behaviour of a joint. For this reason, among others, increasing attention is being given to the so-called strut-and-tie model[5] as a basis for the design of "discontinuity regions" or "disturbed regions" such as joints. With this simple model, the flow of forces in a joint is easily visualized, satisfaction of the requirements of equilibrium is confirmed, and the need for proper anchorage of bars is emphasized. In a complete strut-and-tie model analysis, through proper attention to deformations within the joint, serviceability is ensured through control of cracking.

The strut-and-tie model not only provides valuable insights into the behavior of ordinary beam-column joints but also represents an important tool for the design of joints that fall outside of the limited range of those considered [6]. Further

development of joint design methods may well incorporate this approach. The strut-and-tie model of Fig.(4) provides valuable insight into the needed reinforcement, indicating that, in addition to well-anchored tensile bars to transmit the force T into the joint, some form of radial reinforcement is required to permit the compressive force C to "turn the corner".
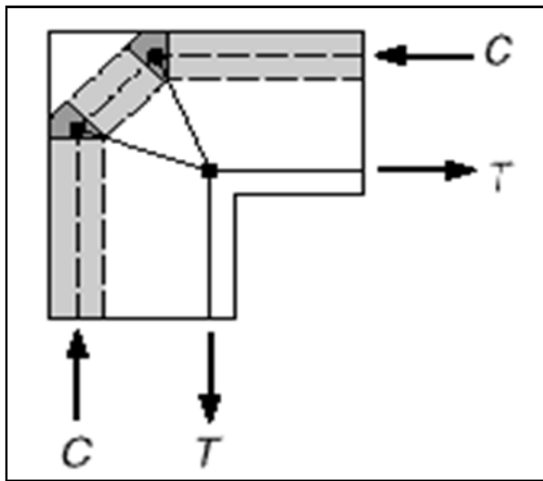

Fig.4 Strut-and-tie Model of Joint Behaviour.[3]

3. Requirements Regarding Reinforcement Layout:

The reinforcement should be placed in such a way that the joints meet certain basic requirements:[2]

1. The joint should be capable of resisting a moment at least as large as the calculated failure moment in adjacent cross section, i.e., begins yielding in the beam reinforcement. Consequently, failure in the joint does not occur and the structure is able to develop its computed strength.
2. If it is not possible to meet the first requirement, then the reinforcement layout should satisfy a second requirement. The joint should have the necessary ductility to carry large deformations so that redistribution of forces in the structure will be possible without brittle failures of joints. In

statically determinate structures, such as bridge abutments, retaining walls and open channels, there is no redistribution of moments to adjacent structural elements. In such case the strength of the corner is critical for integrity of the structure.
3. Cracks form on the inside of corners which are subject to tension. The widths of corner cracks should, therefore, be limited to an acceptable value in the working range .
4. The reinforcement should be easy to fabricate and position. Corners and joints are often of considerable width. For such joints, details, which include stirrups, may be difficult to place in practice, and care must be taken that the reinforcement does not seriously disturb the casting of the concrete.

4. Material Models:

Concrete behavior is simulated by the elastic-plastic model with a five-parameter William-Warnke[7] failure surface. The failure surface consists of a conical shape with curved meridians and noncircular base sections, it is defined as:

$$\frac{1}{z}\frac{\sigma_a}{f_{cu}} + \frac{1}{r(\theta)}\frac{\tau_a}{f_{cu}} = 1 \ldots.(4)$$

Where, σ_a and τ_a are the average stress components, r is the position vector locating the surface with angle θ, z is the apex of the surface and f_{cu} is the uniaxial compressive strength. The free parameters of the surface z and r are identified from uniaxial compressive strength f_{cu}, biaxial compressive strength f_{cb}, and uniaxial tensile strength f_{ct}. The William-Warnke failure surface has several advantages which include: close fit of experimental data in the operating range; simple identification of model parameters from standard test; smoothness; and convexity. In order to guide the expansion of the yield surface during plastic deformation, the

uniaxial stress-strain relationship for normal-strength concrete is defined as [8]

$$\sigma_c = \frac{E_c \, \varepsilon_c}{1+(\frac{\varepsilon_c}{\varepsilon_0})} \quad \ldots(5) \qquad \varepsilon_0 = \frac{2f_c'}{E_c} \quad \ldots(6)$$

$$E_c = \frac{\sigma_c}{\varepsilon_c} \qquad\qquad \ldots(7)$$

$\sigma_c =$ stress at any strain ε, $\varepsilon_c =$ strain at stress σ, $\varepsilon_0 =$ strain at the ultimate compressive strength f_c'. The relationship is approximated by several piecewise linear segments Fig.(5) and the resulting sets of points are incorporated in the material model for concrete. The steel is assumed to be an elastic-perfectly plastic material, identical in tension and compression.
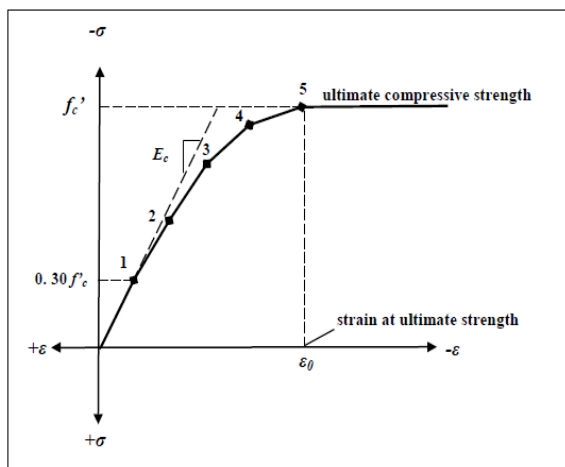
Fig.5 Adopted Stress-Strain Relationship for Concrete in Compression.[8]

5. Applications:

Two case studies are considered for non-linear finite element analysis. Case No.1 refers to the experimental program conducted by Nilsson and Losberg[2], Case No.2 refers to Singh and Kaushik[9].

6. Experimental Test Specimens:

The shape, dimensions and loading arrangement of the test specimens for both case studies are shown in Fig.(6). The portal type shape was selected because of the ease of testing which it affords (the
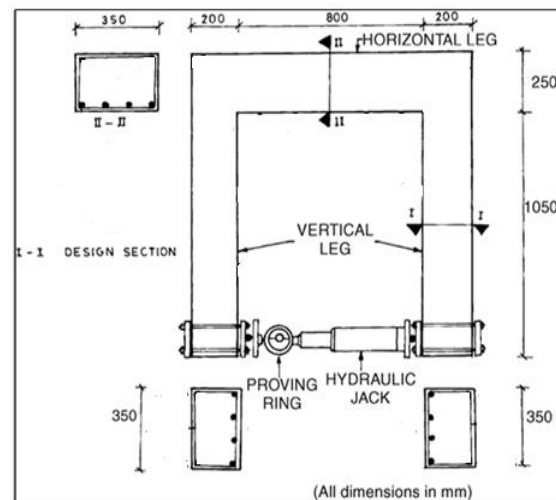
Fig.6 Dimensions and Method of Loading of Test Model.[2], [9]

specimen testing in horizontal position, lying on frictionless supports on the ground) and the two 90° corners allowing for cross-checking of results. The length of the leg was made large enough to ensure flexural failure next to the beam without any risk of the load increasing shear failure. The specimens reproduce well the actual load conditions on practical corners subjected to opening moments. All the corner joint specimens are reinforced with four longitudinal bars in the tension side and are without reinforcement in the compression zone. The four reinforcement details investigated for Case No.1 are: hairpin, simple, loop, and detail with stirrups, which are shown in Figs. (7) to (10). The corresponding bar diameters and material properties are outlined in Table (1). In Case No.2 the reinforcement details investigated are: simple, detail with stirrups, small loop and large loop which are shown in Figs.(11) to (14), 12 mm dia. bars were used for all specimens with a tensile reinforcement ratio equal to 0.76%. Poisson's ratio for concrete was 0.18 for all models investigated and the shear transfer coefficient β_t which represents conditions

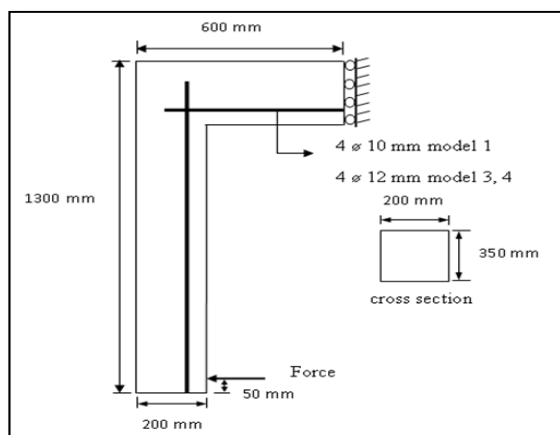of the crack face was equal to 0.3, with no convergence problems encountered.

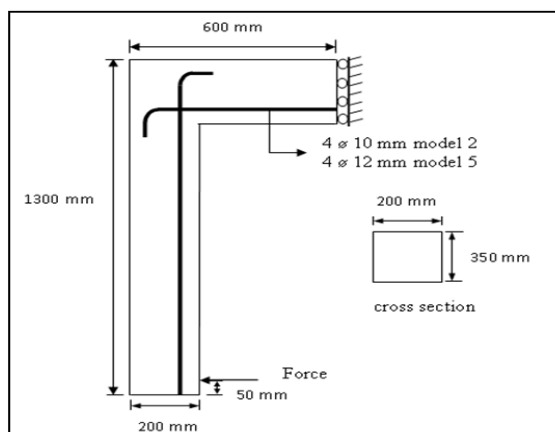**Fig.7 Hairpin Reinforcement Details (H1A,H1B,H1C).[2]**

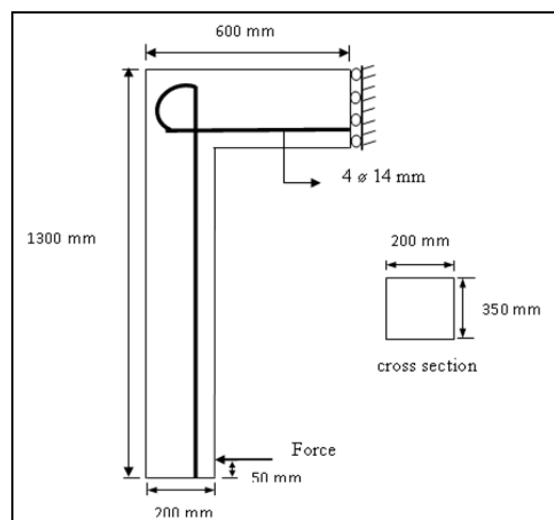**Fig.9 Loop Reinforcement Detail (L1).[2]**

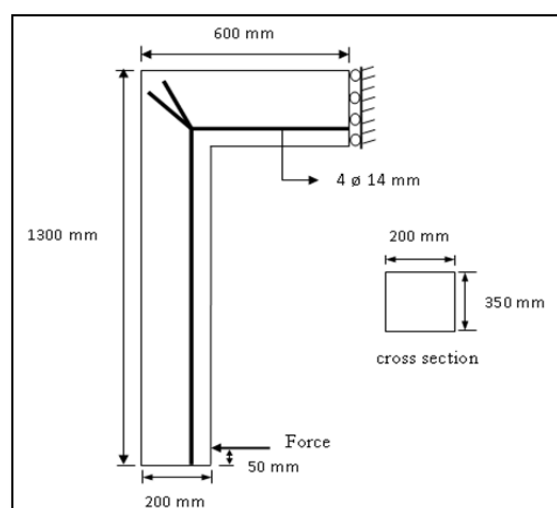**Fig.8 Simple Reinforcement Details (S1A).[2]**

Fig.10 Reinforcement Detail with Stirrups (ST1).[2]

Table (1) Material Properties for Case No.1[2]

Detail Type	Designation	Bar dia.(mm)	Tensile reinforcement ratio ρ, (%)	Yield stress f_y (MPa)	Comp. strength f'_c (MPa)	Modulus of elasticity for concrete E_c(MPa)	Tensile strength of concrete $f_r=0.62\sqrt{f'_c}$
Hairpin	H1A	10	0.5	390	30	25750	3.4
	H1B	12	0.75	390	28	25029	3.28
	H1C	12	0.75	390	28	25029	3.28
Simple	S1A	10	0.5	390	30	25750	3.4
Loop	L1	14	0.75	390	32	26756	3.51
Stirrups	ST1	14	0.75	390	30	26756	3.4
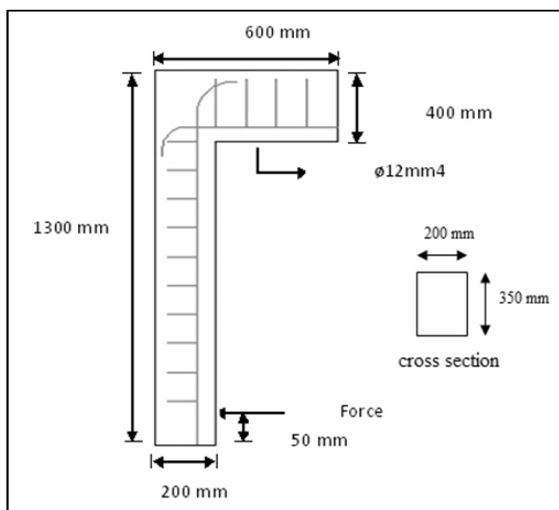
Fig.11 Simple Reinforcement Detail (S2).[9]
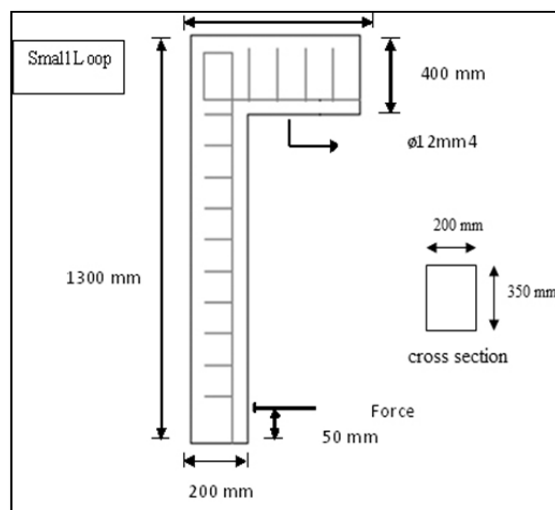
Fig.13 Small Loop Reinforcement Detail (SL2).[9]
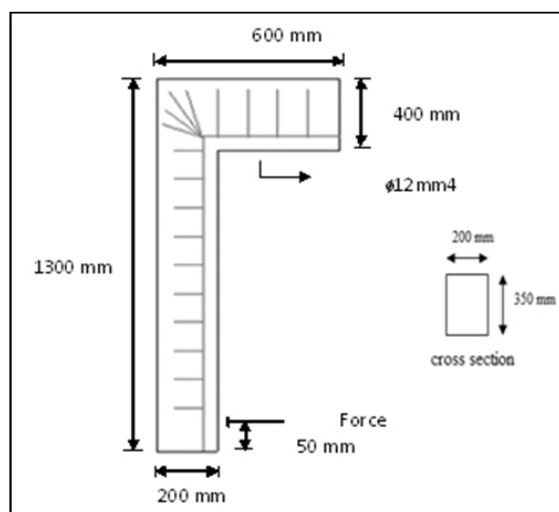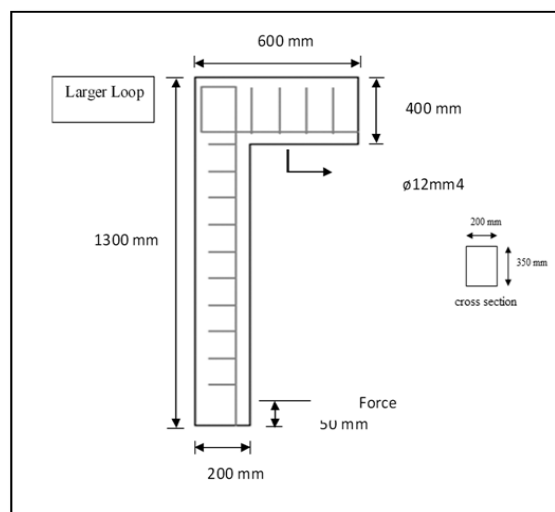

Fig.12 Reinforcement Detail with Stirrups (ST2).[9]

Fig.14 Large Loop Reinforcement Detail (LL2).[9]

Table (2) Material Properties for Case No.2[9]

Detail Type	Designation	Bar dia.(mm)	Tensile reinforcement ratio ρ, (%)	Yield stress f_y (MPa)	Comp. stress f_c' (MPa)	Modulus of elasticity for concrete E_c(MPa)	Tensile strength of concrete $f_r=0.62\sqrt{f_c'}$
Simple	S2	12	0.76	410	42.51	30643	4.04
Stirrups	ST2	12	0.76	410	32	26587	3.51
Small Loop	SL2	12	0.76	410	41.42	30248	3.99
Large Loop	LL2	12	0.76	410	43.03	30830	4.07

7. Finite Element Model:

The reinforced concrete joint specimens are modeled using a combination of SOLID65 and LINK 8 elements available in the ANSYS 12.0 [10] element library, to represent the concrete and steel reinforcement, respectively. The SOLID65 element is an eight node quadrilateral element with three degrees of freedom at each node corresponding to translations in the x, y, and z directions. The element is capable of plastic deformation, cracking in the three orthogonal directions, and crushing. The LINK 8 element is a two-node uniaxial element with three degrees of freedom at each node corresponding to translations in the nodal x, y, and z directions; the element is also capable of plastic deformation.

The nodes of the link elements discretizing the steel reinforcement are aligned to coincide with the corresponding nodes of the solid elements idealizing the concrete, the coincident nodes are then "merged" and the lower numbered coincident node is retained, thus full connectivity is provided between the two types of elements. The corner joint model is symmetric about two planes, therefore only one-quarter of the corner joint need be analysed with corresponding boundary conditions enforced on the two planes of symmetry. The quarter model is illustrated in Fig.(15). The total number of nodes included in the model is 5224 for each of the two cases considered. The models corresponding to the detailing schemes in the study are shown in Figs. (16) to (24). The solution is obtained using the Newton-Raphson procedure with 20 substeps and a maximum number of iterations equal to 100.
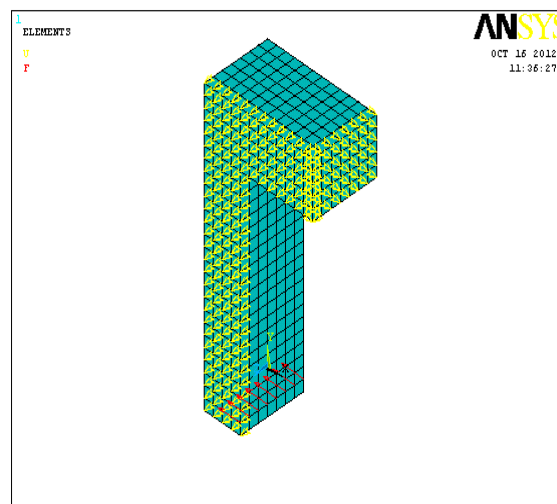

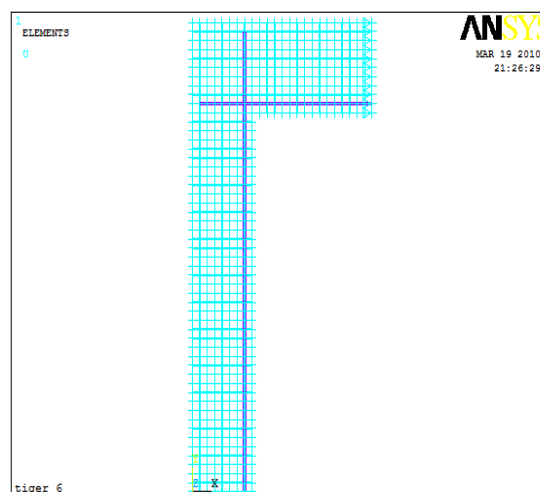**Fig.15 Finite Element Model of Corner Joint: 3-Dimensional View.**
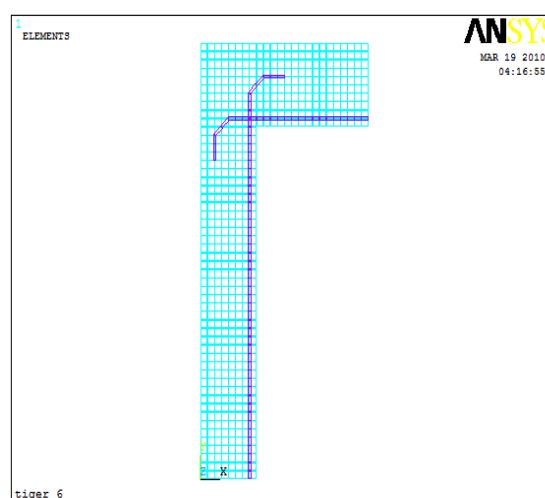

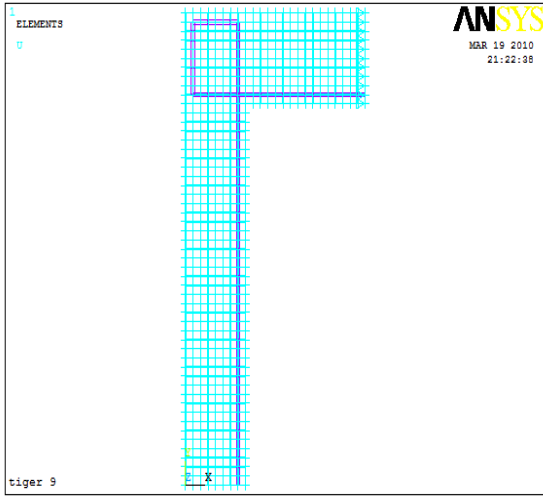**Fig.16 Finite Element Models H1A,B,C.**

Fig.17 Finite Element Model S1A.

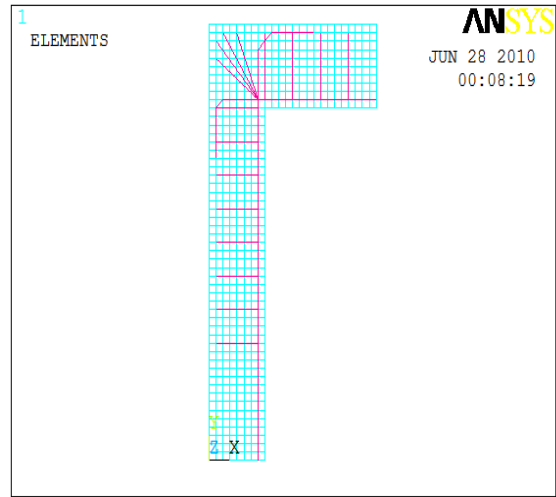**Fig.18 Finite Element Model L1.**

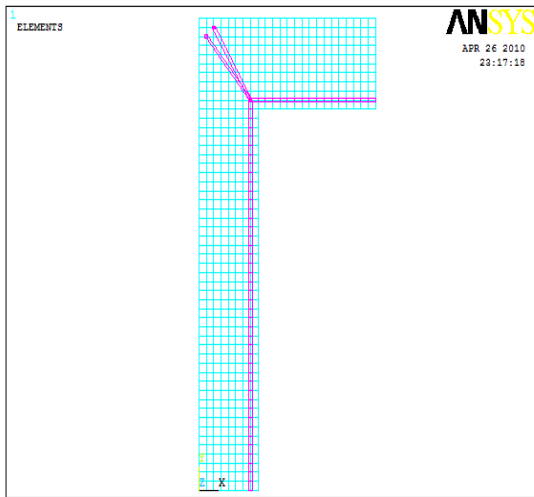**Fig.21 Finite Element Model ST2.**
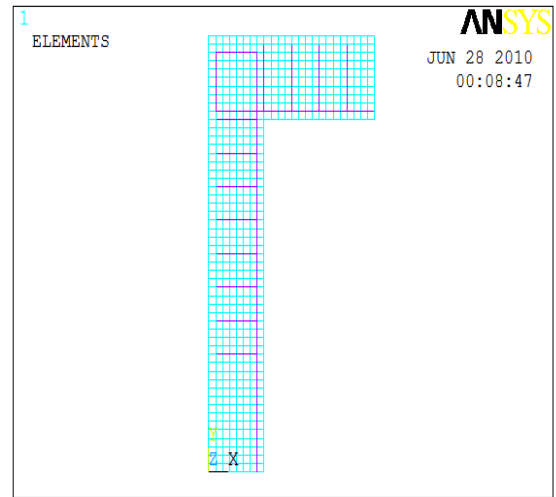

Fig.19 Finite Element Model ST1.

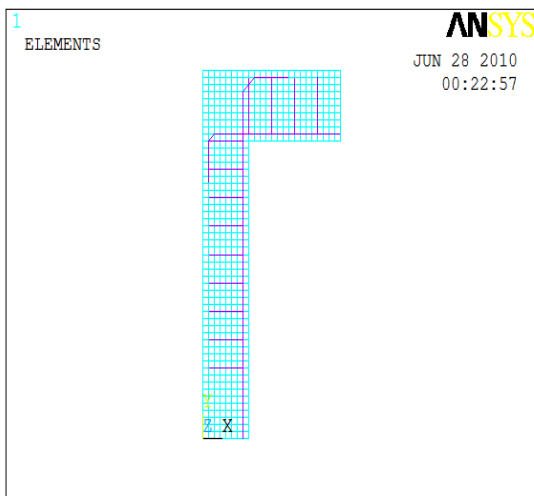**Fig.22 Finite Element Model SL2.**

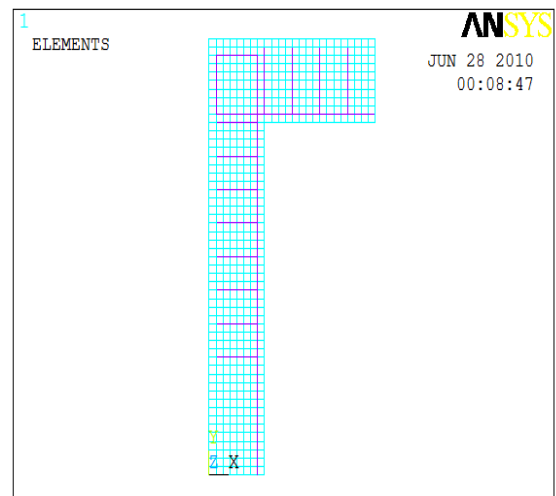**Fig.20 Finite Element Model S2.**

Fig.23 Finite Element Model LL2.

8. Discussion of Results:

Case No.1

Models H1A, B and C (Hairpin Detail)
The models H1A, H1B and H1C were reinforced with bent bars in the form of hairpins. Failure was initiated by the occurrence of a diagonal crack that caused the portion of the corner outside a line through the anchored bends to be pushed off. The diagonal crack and idealization of corner is shown in Fig.(3). It is seen that an increase in the steel reinforcement ratio results in a lower joint efficiency. The crack pattern evolution for model H1A, and at failure only for models HIB, H1C is shown in Figs. (24) and (25).

Models S1A (Simple Detail) Model S1A is reinforced as shown in Fig.(8). On loading to failure, the same type of cracking occurred in the corners Fig.(3), the portion of the corner outside the bent reinforcement was pushed off due to diagonal tension crack failure. Failure occurred suddenly with the ultimate load capacity for the model remaining about constant and independent of the reinforcement ratio. The same observation is made concerning the relation between the reinforcement ratio and joint efficiency as in the preceding detail (Hairpin). Fig.(25) depicts the corresponding crack pattern at failure.

Model L1 (Loop Detail) An old way of placing the reinforcement in a corner, which is often used, is to form it into a loop. This arrangement was tested in specimen L1. At application of load , a wide corner crack occurred which under further loading branched and followed the reinforcement loop out into the corner until the crack surrounded the whole loop. At an increased load level the portion of the corner outside the loops was finally pushed off. This is shown in Fig.(25).

Model ST1 (Detail with Stirrups) Corner reinforcement details with the addition of stirrups are often referred to in available literature. In an attempt to resist the tensile stresses, σ_y, and thereby prevent spalling of the corner, the joint was augmented by stirrup reinforcement. On application of the load, failure occurred in the corner. Failure was not preceded by reinforcement yielding in the corner, but was caused by an insufficient arrangement of the reinforcement. The stirrups increased the strength and ductility of the corner. However, the use of stirrups in corners and joints of long length, as between walls and slabs, is usually a technically undesirable solution due to the practical difficulties of placing and casting. Fig.(25) shows the crack pattern at failure.

A comparison with experimental results for the above models is outlined in Table (3), the Table also shows that the joint efficiency for the given models is in descending order. Fig.(26) depicts the load-displacement relationship for all the detailing models considered for the analysis in Case No.1. It is seen that model H1B (Hairpin) shows best results in terms of serviceability, whereas model S1A (Simple) is least efficient in this respect.

Case No.2

Model S2 (Simple Detail) The behaviour at the early stages of loading was elastic until the appearance of the first crack. Invariably the crack was initiated as expected at the re-entrant corner and the crack gradually progressed for some distance along the corner diagonal as the loading progressed. In model S2, the initial crack at the re-entrant corner progressed along the main reinforcement, bent from one member into the other, and then branched out towards the compression zone of the corner until the outer portion of the corner had a tendency to be pushed out and get detached. The corner was characterized by efficiency as low as 58%.
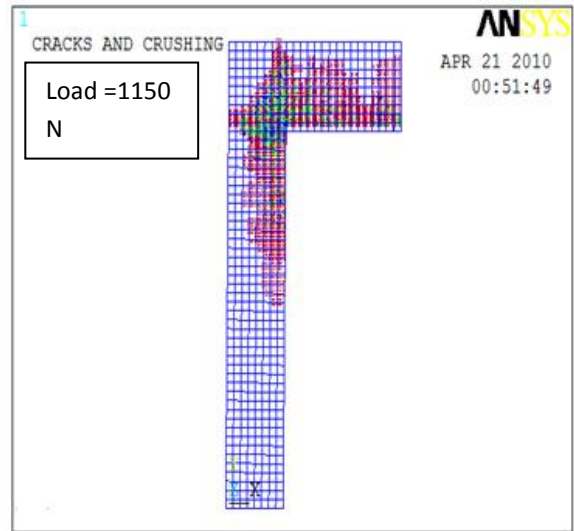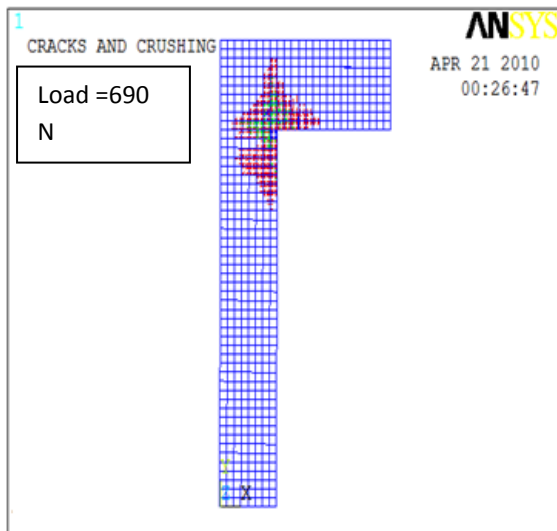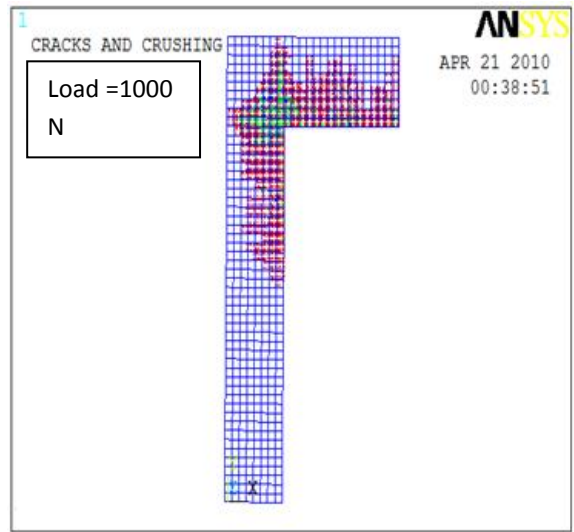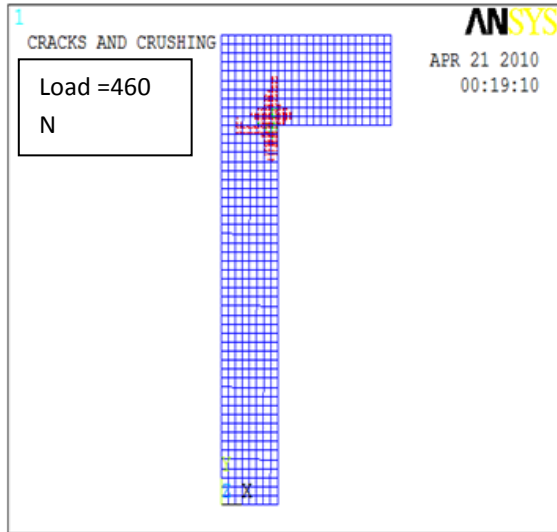
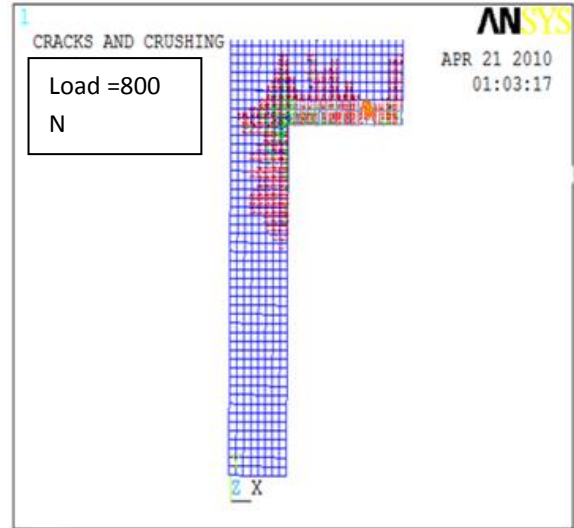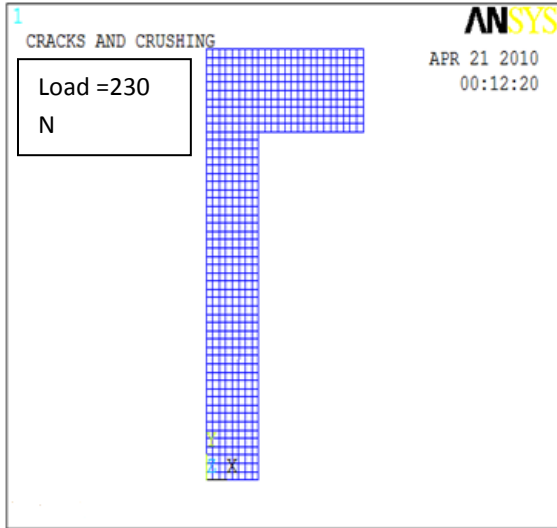**Fig.24 Evolution of Crack Patterns for Model H1A(Hairpin).**

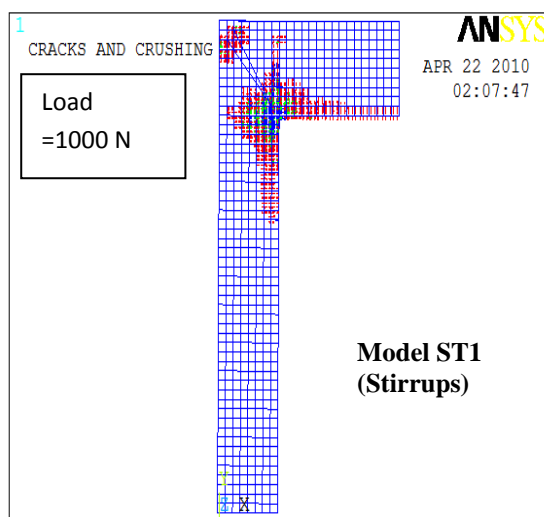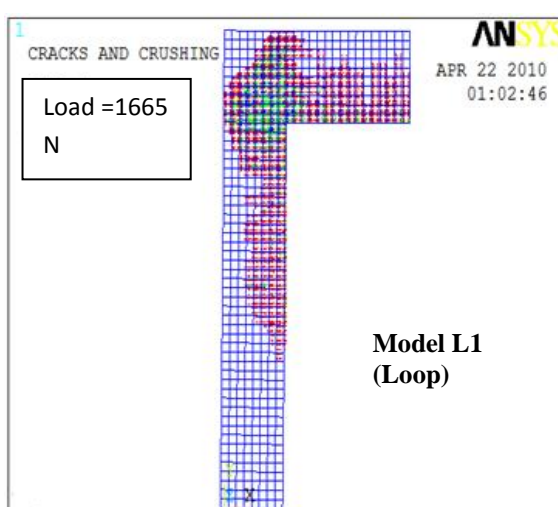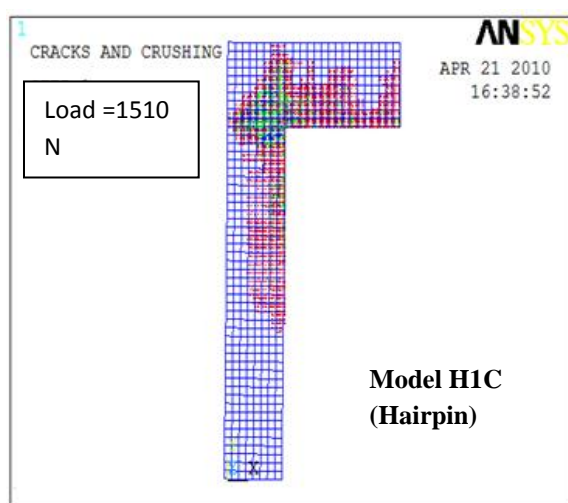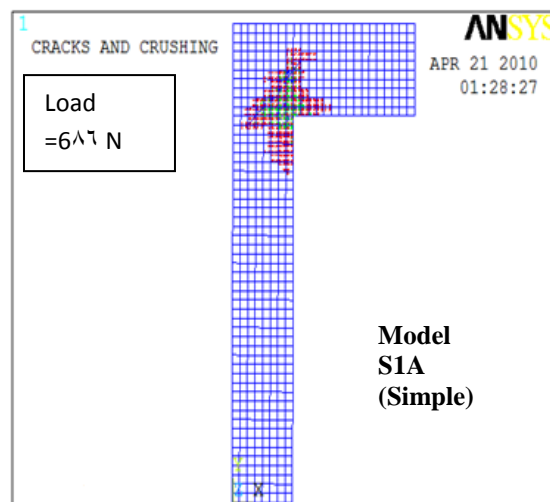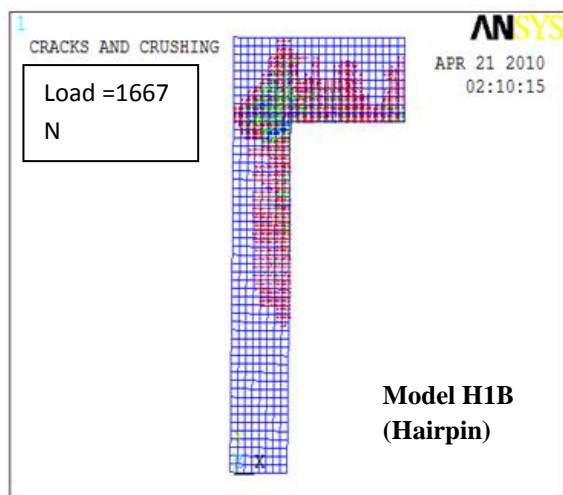**Fig.(25) Crack Patterns at Failure for Models H1B, H1C, S1A, L1, ST1**

Table (3) Comparison of Results for Case No.1

Designation of Corner	Force at first crack (N)	$P_{ansys.}$ (N)	$P_{exp.}$[2] (N)	P_{cal} (N)	P_{cal}/P_{exp}	$P_{ansys.}/P_{exp.}$	$M_{ansys.}/M_{cal.}$ (corner efficiency)%
Model H1A	325	1150	1081	781.15	0.72	1.06	147%
Model H1B	300	686	629.24	620.5	0.99	1.08	115%
Model S1A	410	1661	1370	1487.5	1.08	1.19	111%
Model H1C	405	1514	1521	١٦٤٥	1.08	1	92%
Model L1	270	1665	1513	1979.65	1.31	1.08	84%
Model ST1	368	1000	1130	1838.55	1.63	0.88	54%

P_{ansys}: Ultimate load predicted by ANSYS.

$P_{exp.}$: Ultimate load from experiments.

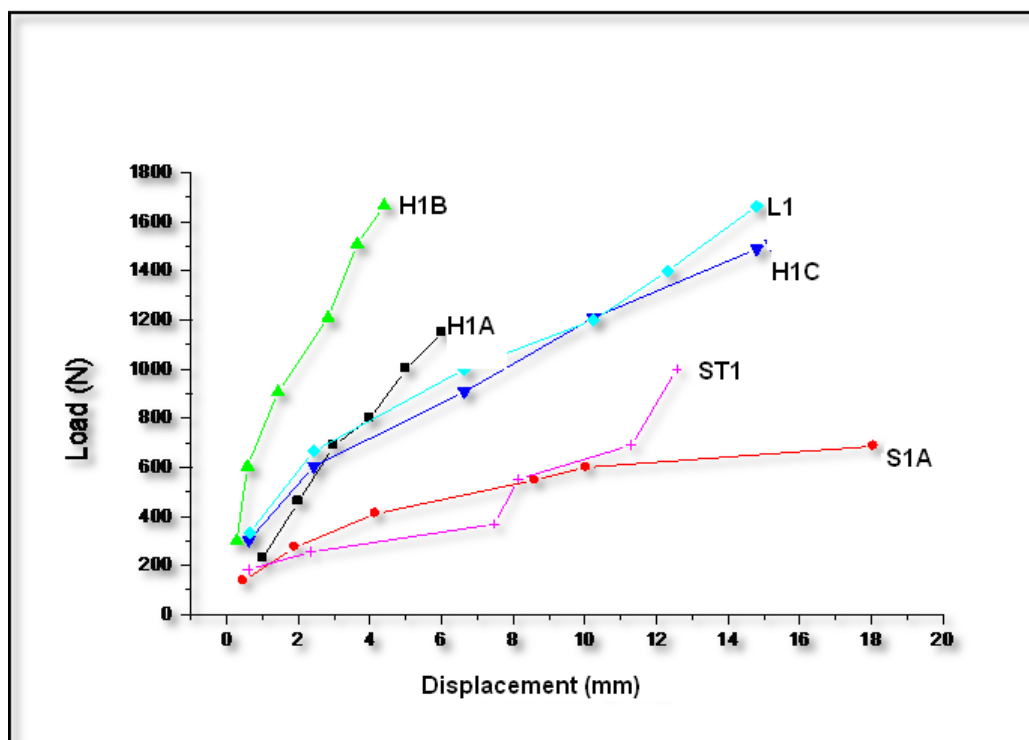$P_{cal.}$: Ultimate load calculated from eq.(3)

Fig.(26) Load-Displacement Curve (ANSYS) for Models (Case No.1)

The unexpectedly low efficiency of this widely used detailing method can be explained by the fact the corner has no capacity to carry the resulting tensile forces induced due to external loading. It is evident that the structural characteristics of the corner are controlled by tensile strength of concrete in the absence of an alternate mechanism to carry the tensile forces. The mode of failure of model S2 suggests that a mechanism to carry the induced diagonal tensile force would result in higher efficiencies. The crack pattern evolution is depicted in Fig.(27).

Model ST2 (Detail with Stirrups) Consequently in model ST2, two legged closed stirrups aligned along the corner diagonal as far as possible were introduced Fig.(١٢). Significant improvements in behaviour were observed in model ST2 upon loading. The stirrups were apparently effective in carrying a significant amount of diagonal tension and the joint efficiency increased to 77%. The crack widths at service loads were not reduced and there was an increase in the extent of cracking. It may by noted that the joint efficiency was still below 100% in spite of the provision of a primary diagonal tension-resisting element in the form of stirrups. For the stirrups to be effective, it is imperative that these be wrapped around the main steel in the corner as closely as possible so that the concrete need not undergo unduly large strains before the tensile load is transferred to stirrups. As load increases the strain increases and the crack evolves in the re-entrant and the two legs. The results discussed above are shown in Fig.(٢٨).

Model SL2 (Small Loop Detail) Corner reinforcement in the form of loops as shown in detailing system model SL2, Fig.(٢٢), has been for quite some time considered as the most obvious way of altering the direction of a rebar situated on the inside face of angle shaped concrete structures. On loading the model , a wide corner crack occurred, which on further

loading, split and closely followed the rebar loop out into the corner until this circular crack encircled nearly the whole loop. The formation of this nearly circular crack encompassing the loop suggests that the loop has apparently exerted some confining pressure on the concrete within the loop. Model SL2 had an efficiency of 104%. This exceptional structural behavior of the corner may be attributed to the detailing characteristics of this model in which the geometry of the rebar loop has been effective in filling the corner as much as possible and hence, enclosing a large part of the concrete in the joint. The confining pressure exerted by the loop closing under external load has apparently increased the tensile strength of the concrete within the loop. On further application of the load, the portion of the corner outside the loop had a tendency to be pushed out resulting in failure of the specimen. Fig.(28) depicts the crack pattern at failure.

Model LL2 (Large Loop Detail) Detailing system model LL2 is a more practical variant of the loop reinforcement tried in the above model. It is achieved through the use of two bent bars; the bar in each leg of the specimen is brought well inside the corner and then bent back into the compression zone of the same leg. This detail offers the advantage that the two bent bars enclose the corner with reinforcement better than the small loop detail. Under loading, the crack in the model was initiated at the re-entrant corner as usual and on subsequent loading, the crack travelled along the corner diagonal for some distance and then branched out into numerous cracks progressing towards the compression zone of the corner. The final stages were marked by the appearance of a crack near the exterior portion of the corner the joint aligned more or less perpendicular to the corner diagonal, Fig.(28). The model indicated an
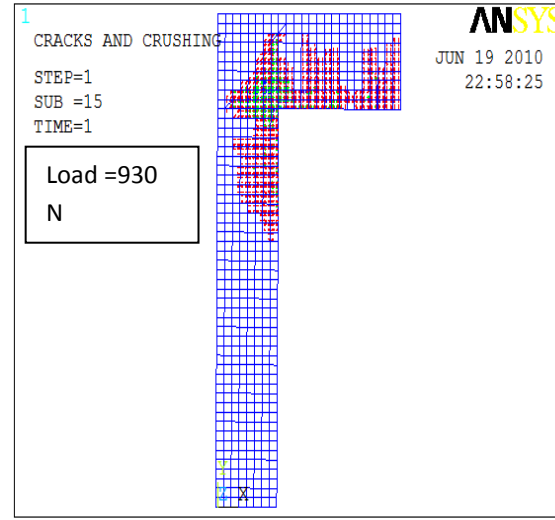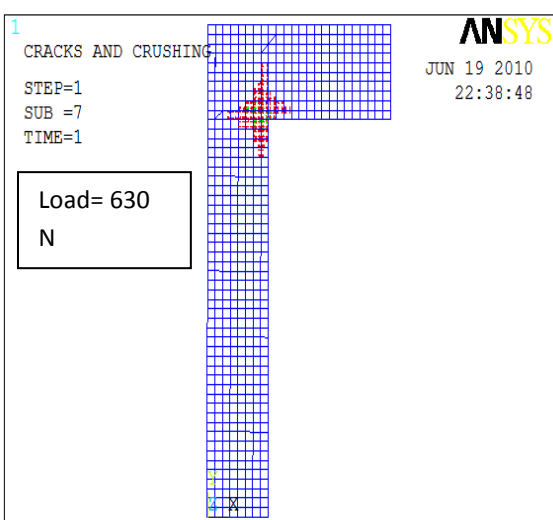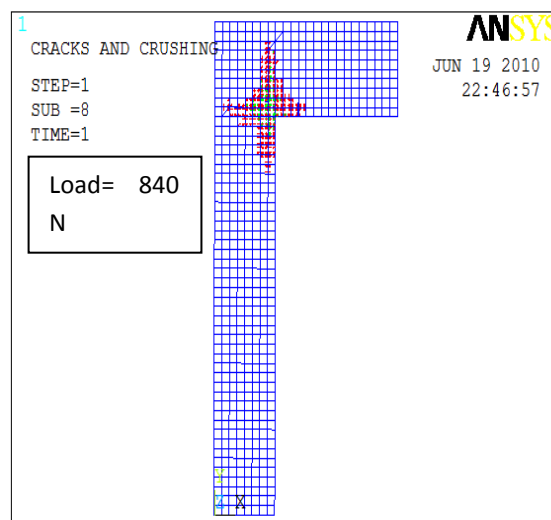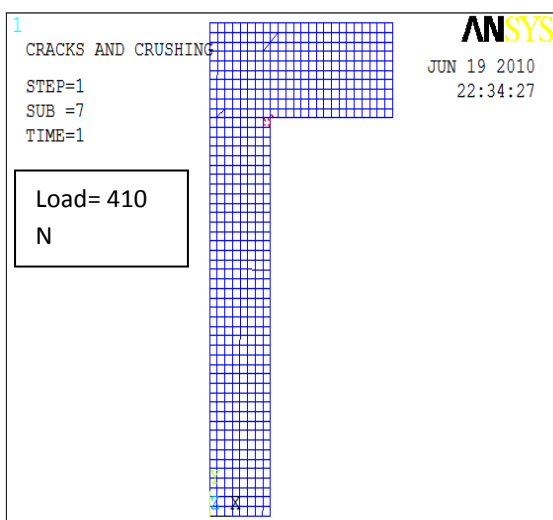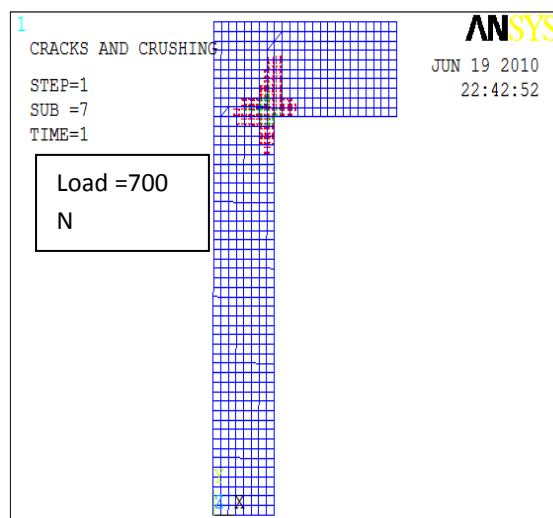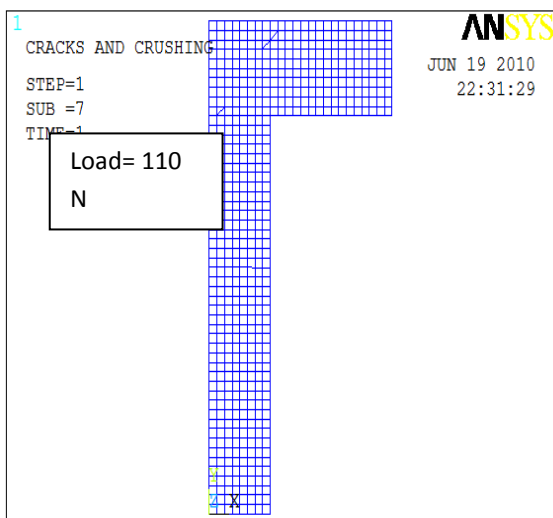
Fig.(27) Evolution of Crack Patterns for Model
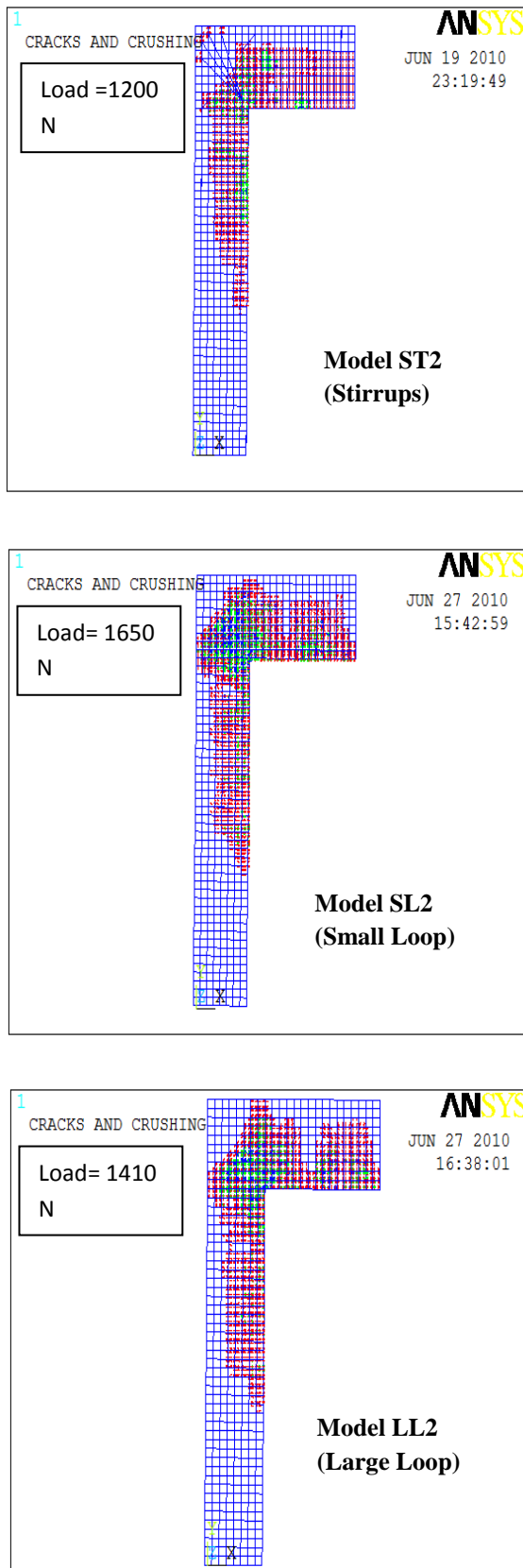
S2 (Simple Detail)

**Fig.(28) Crack Patterns at Failure
for Models ST2, SL2, LL2**

Table(4) compares the results obtained in Case No.2 with experimental values and indicates the relative joint efficiencies for the given detailing systems. Fig.(29) depicts the load-displacement relationship for all the detailing models considered for analysis in Case No.2. It is evident that model ST2 (Stirrups) shows best results in terms of serviceability, exhibiting minimum displacement among models for the same load level.

9. Conclusions:

1- The three-dimensional nonlinear finite element model, which was adopted in the present work, is suitable for predicting the behaviour of the reinforced concrete joints subjected to non-proportional monotonically increasing loading. The numerical results were in good agreement with experimental results throughout the entire range of behaviour.

2- The corner joint behaviour is highly influenced by the detailing configurations.

3- The hairpin detail showed an efficiency range of 92-147% with higher joint efficiency at lower reinforcement ratios.

4- The simple detail showed efficiencies of 58-111% with a similar observation as above relating to the reinforcement ratio.

5- The addition of stirrups to the simple detail resulted in 54-77% efficiencies. The practical difficulties involved with the placement and fixing of the stirrups may discourage their use, especially in deep members.

6- The small loop detail showed an efficiency of 104% but is difficult to fabricate. An easier alternative is the large loop with a slightly lower efficiency of 91%.

Table (4) Comparison of Results for Case No.2

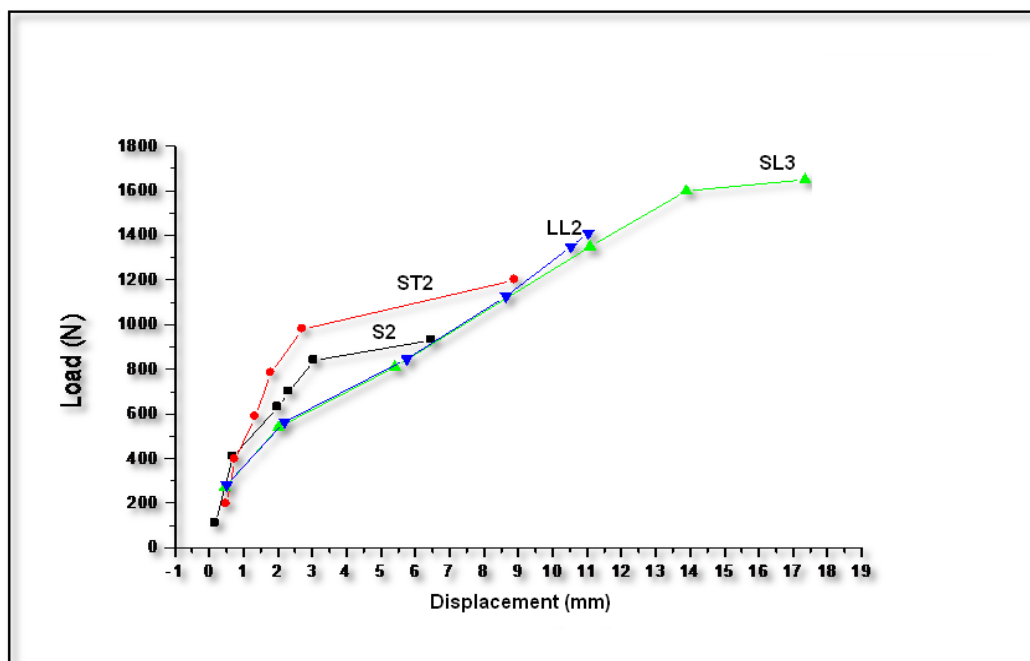| Designation of Corner	Force at first crack (N)	P_{ANSYS} (N)	$P_{exp.}$ [9] (N)	P_{cal} (N)	P_{cal}/P_{exp}	$P_{ansys}/P_{exp.}$	$M_{ansys}/M_{cal.}$ (corner efficiency) %
Model SL2	320	1650	1769.73	1591.2	0.90	0.94	104%
Model LL2	350	1410	1470	1558.1	1.06	0.96	91%
Model ST2	396	1200	1248.75	1552.5	1.24	0.96	77%
Model S2	410	930	805.62	1595	1.98	1.15	58%

Fig.(29) Load-Displacement Curve (ANSYS) for Models (Case No.2)

10. References:

[1] Park, S. and Mosalam, K. "Experimental Investigation of Non-Ductile Reinforced Concrete Corner Beam-Column Joints with Floor Slabs." Journal of Structural Engineering, ASCE, accepted for publication, posted ahead of print 22 Feb. 2012.

[2] Nilsson, I. H. E and Losberg, A. "Reinforced Concrete Corners and Joints Subjected to Bending Moment." Journal of the Structural Division, ASCE, vol 102, No. 6, 1976, pp 1229-1253.

[3] Nilson, A.H., Darwin, D., and Dolan, C.W. "Design of Concrete Structures", 13th Edition, McGraw-Hill Book Company, (2004).

[4] "Recommendations for Design of Beam-Column Joints in Monolithic Reinforced Concrete Structures" Reported by ACI Committee 352, ACI Struct. J., Vol. 82, no. 3, 1985, pp. 266-283.

[5] "Building Code Requirements for Structural Concrete and Commentary", Appendix A, ACI 318-02 and ACI 318R-02, American Concrete Institute, Farmington Hills, MI, 2002.

[6] Hamahara, M. et al. "Design for Shear of Prestressed Concrete Beam-Column Joint Cores.", Journal of Structural Engineering, ASCE, vol.133, No.11, (Nov.2007), pp1520-1530.

[7] Chen, W. F. "Plasticity in Reinforced Concrete", McGraw-Hill Book Company, 1982.

[8] MacGregor, J.G. "Reinforced Concrete Mechanics and Design", Prentice-Hall, Inc., Englewood Cliffs, N.J.,(1992).

[9] Kaushik, S.K. and Singh B. "Investigations on Fibre Reinforced concrete Opening Corners", IE (I) Journal-CV, Vol.84, November 2003, pp 201-209.

[10] SAS, ANSYS 12.0, "Finite Element Analysis System", SAS IP, Inc, (2009).